Supporting Information

Structural and Interfacial Characterization of a Sustainable Si/Hard Carbon Composite Anode for Lithium-ion Batteries

Leonardo Sbrascini,[†] Antunes Staffolani,[†] Luca Bottoni,[†] Hamideh Darjazi,[†] Luca Minnetti,[†] Marco Minicucci,[‡] and Francesco Nobili [†,⁑]*

[†]School of Science and Technologies – Chemistry Division, University of Camerino, 62032 Camerino, Italy

[‡]School of Science and Technologies – Physics Division, University of Camerino, 62032 Camerino, Italy

[⁑]GISEL – Centro di Riferimento Nazionale per i Sistemi di Accumulo Elettrochimico di Energia, INSTM, 50121 Firenze, Italy

*Corresponding author. E-mail: leonardo.sbrascini@unicam.it

KEYWORDS: Lithium-ion battery, Silicon composite anode, Hard carbon, Ex-situ Raman spectroscopy, Impedance spectroscopy, Interfacial characterization, Distribution of relaxation times

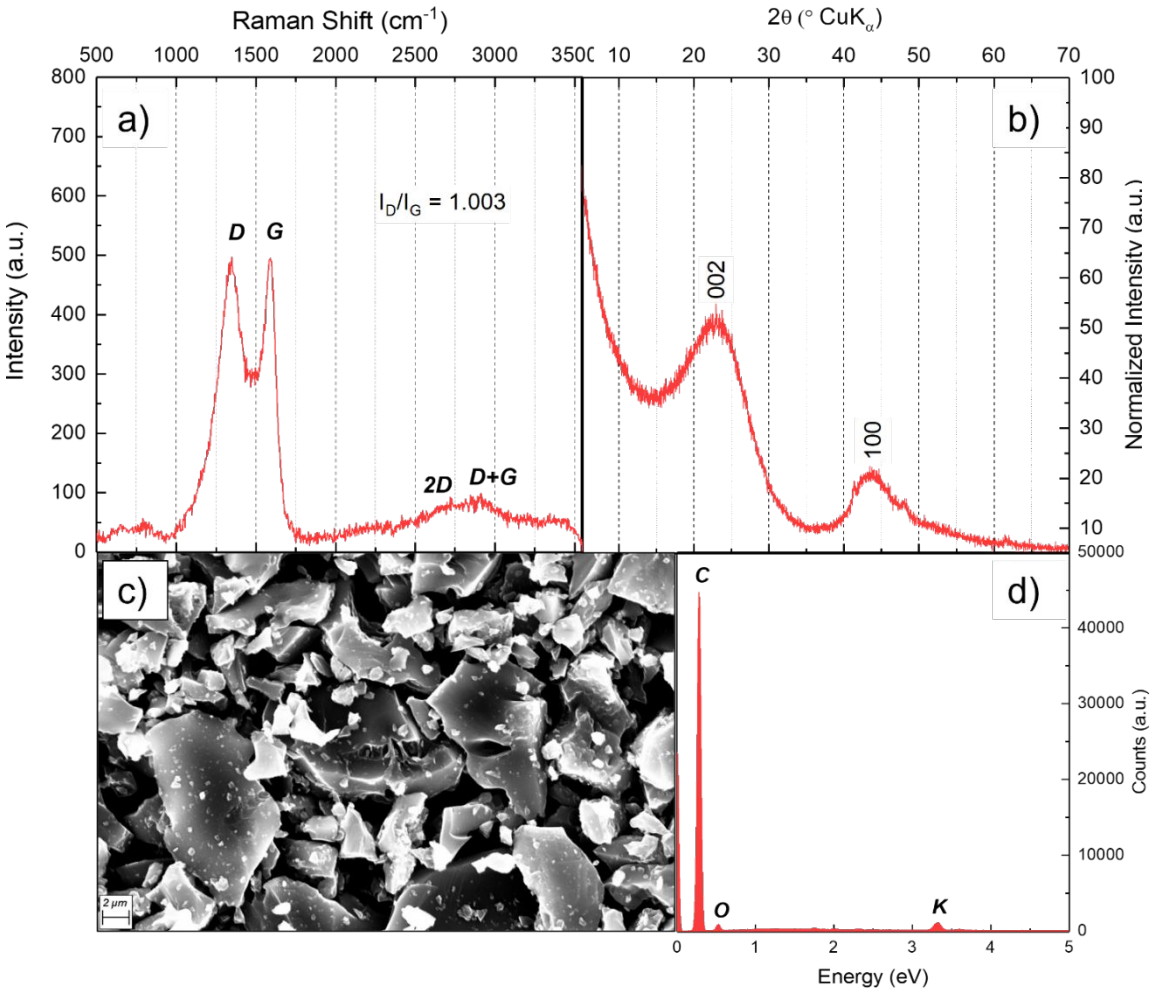

Figure S1. a) Raman spectrum of CCDHC; b) Experimental diffraction pattern of CCDHC; c) SEM micrograph of CCDHC at 5000x magnification; d) EDX analysis of CCDHC.

The equations used for the determination of the structural and crystallographic parameters are listed as follows:

$$L_a = (2.4E^{-10})\lambda^4(I_D/I_G)^{-1} \quad \text{(S1)}$$

with λ = 532 nm;

$$d_{002} = \lambda/2sin\,(\theta_{002}) \quad \text{(S2)}$$

$$L_c = 0.9\lambda/\beta_{002}\cos\,(\theta_{002}) \quad \text{(S3)}$$

with λ = 0.154 nm, and β_{002} = Full Width at Half Maximum (FWHM) of the peak associated to the 002 reflection plane.

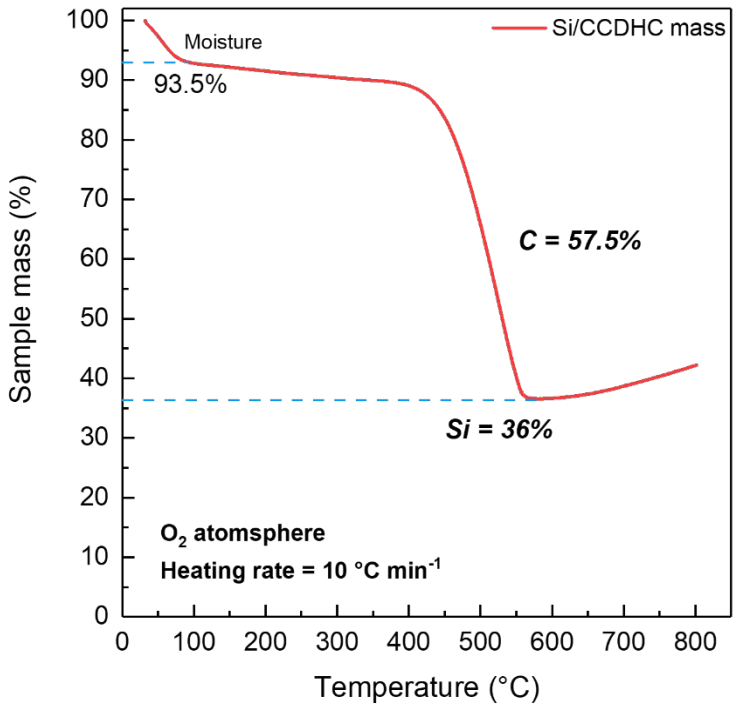

Figure S2. TGA of the Si/CCDHC composite after ball-mill in O_2 atmosphere (heating rate = 10 ˚C min^{-1}; temperature scan range = 30-800 ˚C).

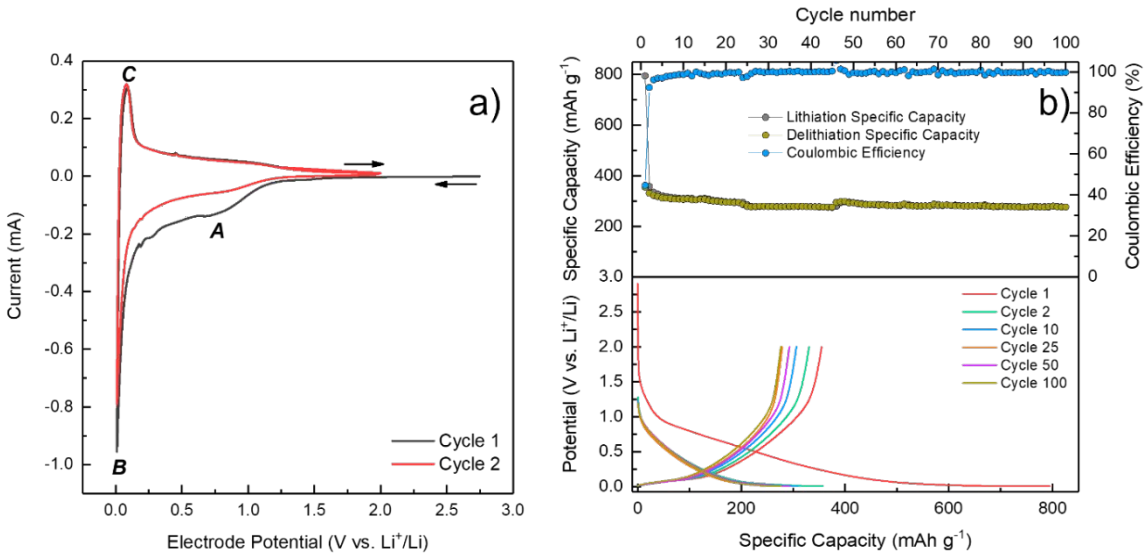

Figure S3. a) Cyclic voltammetry of the first two cycles for the bare CCDHC; b) galvanostatic cycles and E vs Q profiles obtained at 0.3 A g^{-1} for the bare CCDHC.

In **Figure S3a**, a broad signal is present between 0.8 and 0.6 V during the first cathodic scan (peak A), which is due to the electrolyte decomposition on the electrode surface to form the SEI layer. This process is the main cause for the irreversible capacity also displayed in **Figure S3b**. In the following cycles, this peak disappears, meaning the SEI is completely formed. At lower potentials, peak B starts appearing at about 0.1 V. This intense signal is attributed to the intercalation of Li^+ ions between graphene planes. During the first anodic scan, the peak centered at 0.1 V (peak C) can be attributed to the process of de-intercalation of Li^+ ions. For both charge and discharge, the broadened regions above 0.2 V can finally be associated to the

adsorption/desorption of Li from the surface defects of the hard carbon [1]. From the second scan onwards, the voltammograms are superimposed. Notably, despite the high initial irreversible capacity, the coulombic efficiency rapidly rises to values close to 100 %.

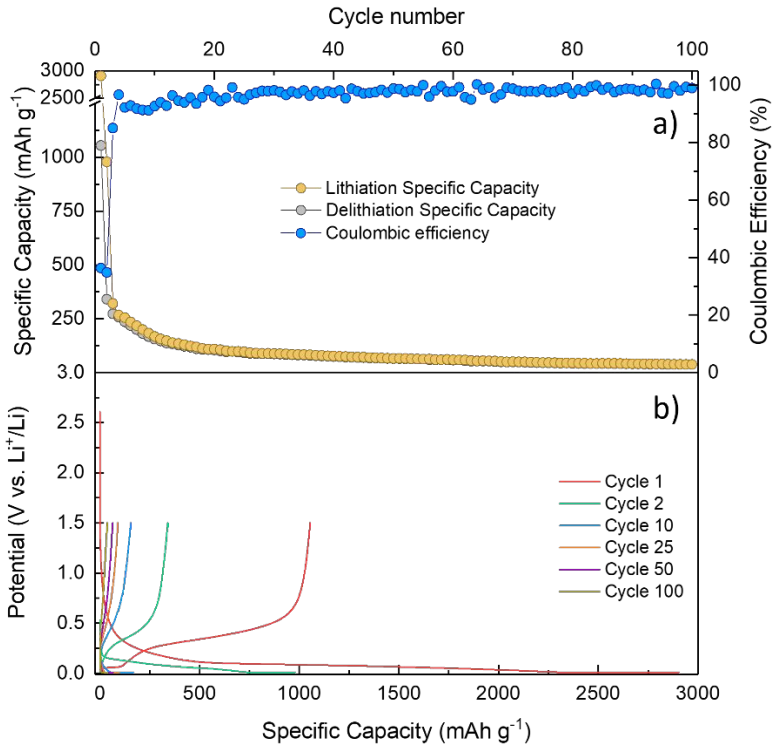

Figure S4. a) Galvanostatic cycles and b) E vs Q profiles obtained at 1.0 A g-1 for bare Si nanoparticles with the CS/CA binder.

In **Figure S4a-b**, the bare Si electrode displays the characteristic decay of capacity due to repeated volume changes upon cycling, starting with a first lithiation yielding a capacity of almost 3000 mAh g-1 but falling to very low values after just few cycles, as a result of

delamination and loss of electrical contact. This result further provides confirmation of the beneficial effect of CCDHC when coupled to bare Si.

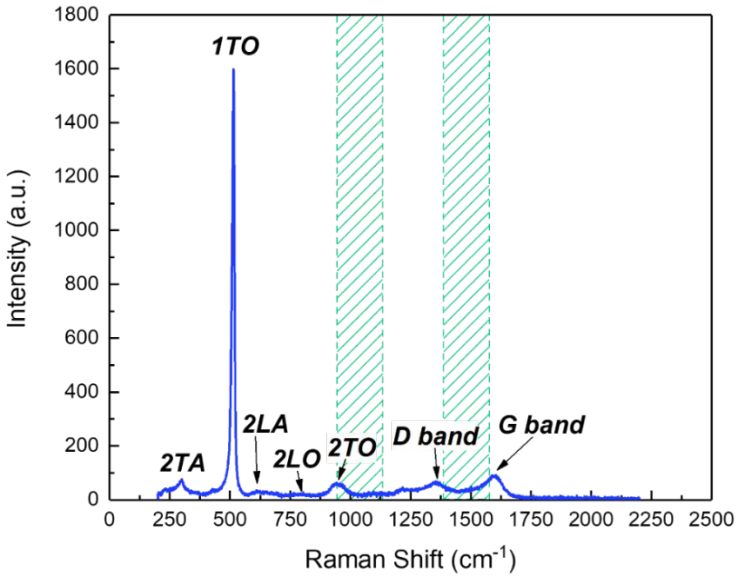

Figure S5. Raman spectrum acquired on the pristine Si/CCDHC electrode evidencing the regions where Chitosan signals are expected.

From the Raman spectrum performed on the pristine electrode, no signals related to Chitosan [2] are detected (green-shaded regions). Hence the signals recorded for the ex-situ measurements are related to the presence of decomposition products from the electrolyte and from the VC additive.

REFERENCES

(1) Wang, N.; Liu, Q.; Sun, B.; Gu, J.; Yu, B.; Zhang, W.; Zhang, D. N-Doped Catalytic

Graphitized Hard Carbon for High-Performance Lithium/Sodium-Ion Batteries. *Sci. Rep.* **2018**, *8* (1), 1–8. https://doi.org/10.1038/s41598-018-28310-3.

(2) Zajac, A.; Hanuza, J.; Wandas, M.; Dymińska, L. Determination of N-Acetylation Degree in Chitosan Using Raman Spectroscopy. *Spectrochim. Acta - Part A Mol. Biomol. Spectrosc.* **2015**, *134*, 114–120. https://doi.org/10.1016/j.saa.2014.06.071.